Available online at www.sciencedirect.com

ScienceDirect

Procedia Structural Integrity 2 (2016) 1055–1062

Structural Integrity Procedia

www.elsevier.com/locate/procedia

21st European Conference on Fracture, ECF21, 20-24 June 2016, Catania, Italy

# The influence of the alpha grain size on internal fatigue crack initiation in drawn Ti-6Al-4V wires

Joris Everaerts*, Bert Verlinden, Martine Wevers

*Department of Materials Engineering, KU Leuven, Kasteelpark Arenberg 44 bus 2450, 3001 Leuven, Belgium*

**Abstract**

In the very high cycle fatigue regime, the location of crack initiation in titanium alloys is known to shift from the surface towards the bulk of the material. This internal fatigue crack initiation results in faceted features on the fracture surface. These facets are in fact alpha grains that have been broken in a planar manner. Typically, a cluster of many facets is observed either just below the surface or deeper inside the bulk. In this study, uniaxial tension-tension fatigue tests are performed on Ti-6Al-4V wires which have been subjected to different heat treatments in order to vary the alpha grain size. Four different microstructures are obtained, with average alpha grain sizes of approximately 1, 2, 5 and 10 µm. The fatigue life is found to decrease with increasing grain size. Electrochemical polishing of the wires prior to fatigue testing is applied in order to promote internal crack initiation at higher stresses and consequently shorter testing durations. Four samples broke due to an internal crack: three samples with average alpha grain size 5 µm, which failed after 2.6 x $10^7$, 5.7 x $10^7$ and 9.6 x $10^7$ cycles, and one sample with average alpha grain size 10 µm, which failed after only 7.6 x $10^6$ cycles. The threshold stress intensity factor range, which is calculated from the size of the facet-containing area, is between 5 and 6 MPa.$m^{1/2}$ for all four samples. Fractographic examination of the facets reveals that they are not smooth, but show roughness at the nanoscale. This roughness has a linear appearance for nearly all facets, except for one anomalous facet in the sample with the largest grain size, which shows a fan-shaped pattern. From electron backscatter diffraction measurements on cross-sections of the fracture surfaces obtained by focused ion beam milling, it is also found that nearly all the facets coincide with a prismatic plane, and the linear markings are parallel to the prismatic slip direction. Only the anomalous facet has a near-basal orientation. These observations suggest the possibility that facets are formed by either a slip-based mechanism or a cleavage-based mechanism, and that the alpha grain size is one of the parameters that controls which mechanism occurs.


Peer-review under responsibility of the Scientific Committee of ECF21.

*Keywords:* very high cycle fatigue; subsurface crack initiation; fish-eye fracture; quasi-cleavage facets; titanium; Ti-6Al-4V

* Corresponding author. Tel.: +32 16 321234; fax: + 32 16 321990.
*E-mail address:* joris.everaerts@mtm.kuleuven.be

Copyright © 2016 The Authors. Published by Elsevier B.V. This is an open access article under the CC BY-NC-ND license (http://creativecommons.org/licenses/by-nc-nd/4.0/).
Peer review under responsibility of the Scientific Committee of ECF21.
10.1016/j.prostr.2016.06.135

## 1. Introduction

Ti-6Al-4V is an alloy that is frequently used in applications in which fatigue failure is the life-limiting factor, according to Boyer (1996), which is why it is important to understand which mechanisms determine its fatigue behavior. More specifically the crack initiation mechanism must be clarified, because, as mentioned by Kazymyrovych (2009), in the high and very high cycle fatigue regime the initiation phase can take up over 99% of the total fatigue life. Fatigue crack initiation in titanium alloys can occur internally in the gigacyle regime, similarly to fish-eye failure in nickel alloys and high strength steels, as discussed by Bathias et al. (2001). However, titanium alloys generally do not contain inclusions or pores, which are typically the cause of internal cracks. Instead, the initiation area of the fracture surface of internally fractured Ti-6Al-4V samples reveals facetted features, which have been described as having a "cleavage-like" appearance by Paton et al. (1975).

These facets, which are primary α grains that have broken in a planar way, are sometimes termed "quasi-cleavage" facets, although Pilchak et al. (2009) argue that this is not correct because they believe that many cycles contribute to the growth of a facet, which means that there is no cleavage mechanism involved. Therefore they suggest to use the less confusing term "low ΔK faceted growth". In fact, the formation mechanism of α facets has been discussed in many publications, which can generally be categorized in two groups: those who suspect that dislocation slip leads to facets, for example Jha et al. (2012), and those who suspect that facets are formed by cleavage of single α grains, for example Ivanova et al. (2002) and more recently Liu et al. (2016). In any case there seems to be a consensus that the inherent anisotropic nature of the hexagonal α phase, both elastic and plastic, leads to increased localized internal stresses which depend on the local misorientation of neighboring α grains. This has been modeled by Dunne and Rugg (2008), who noted that α grains with certain crystallographic orientations, namely with the c-axis parallel to the loading axis, act as hard grains, while other grains behave as soft grains, because they have a lower elastic modulus and because their orientation facilitates dislocation slip. Neal and Blenkinsop (1976) suggested that dislocations are activated in the "soft" grains and pile up at the grain boundary with a "hard" grain. The stress field caused by the dislocation pile-up leads to cleavage of the latter grain along the normally quoted cleavage plane for the α phase, $\{10\bar{1}7\}$, which lies about 15° from the basal plane . Some evidence of cleavage of α grains has been found by Ivanova et al. (2002), who noticed a fan-shaped pattern, characteristic of a cleavage-type fracture, on a facet. However, many publications argue that it is not cleavage, but localized slip band formation that leads to facets. Bache (1999) provided a possible explanation, in which there is a dislocation pile-up, as described by Neal and Blenkinsop (1976), but instead of cleavage it leads to the formation of a failure slip band in the neighboring "strong" grain. The fact that the facets are sometimes found to be parallel to a prismatic plane of the hexagonal lattice, as was measured by Bridier et al. (2008) for single facets that were the crack origin for surface-initiated cracks, supports this slip-based mechanism.

The effect of the α grain size on internal fatigue crack initiation and facet formation has not yet been thoroughly investigated. In terms of general fatigue life, a large amount of published data was reviewed by Wu et al. (2013) in order to demonstrate that a smaller grain size will lead to a higher fatigue life for both bimodal and equiaxed Ti-6Al-4V. Paton et al. (1975) already suspected that the slip length and thus the grain size would affect the susceptibility of the alloy to form facetted cracks, while Irving and Beevers (1974) noticed that there appears to be a transition from structure sensitive crack growth, with the formation of facets, to a structure insensitive crack growth, and that this transition plausibly takes place when the reverse plastic zone size becomes comparable to the α grain size. Specifically for internal fatigue crack initiation in Ti-6Al-4V, Furuya and Takeuchi (2014) did not find an effect of the grain size on the fatigue life, and they explain this by the fact that the crack origin consists of more than one facet. This means that not the facet size, or equivalently the grain size, but the total size of the cluster of facets determines the fatigue life. This, however, would not make sense if crack initiation and thus the formation of facets takes up most of the fatigue life. The transition from short crack growth, i.e. facet formation, to long crack growth might take place at a constant threshold stress intensity, or equivalently a constant facet cluster size if the stress is not varied, but the stage that dominates the fatigue life is initiation and short crack growth, which is structure sensitive and thus affected by the grain size. This reasoning is confirmed by the results of Oguma and Nakamura (2010), who found that a finer microstructure results in a higher fatigue strength in the VHCF (Very High Cycle Fatigue) regime, and that the α grain

size actually seems to correlate with the occurrence of internal crack initiation, although they only tested two different microstructures and they did not inspect the facets in detail.

The purpose of this paper is to further investigate the effect of the α grain size on the high and very high cycle fatigue behavior of electrochemically polished Ti-6Al-4V wires, with a focus on internal fatigue crack initiation. Four different microstructures are investigated and the fracture surfaces are closely examined. Additionally, focused ion beam milling (FIB) is performed to locally cut through the fracture surface in order to reveal the crystallographic orientation of the facetted grains by electron backscatter diffraction (EBSD) measurements.

## 2. Materials and methods

The Ti-6Al-4V wire (ASTM B863, grade 5), which has a diameter of 1 mm, is supplied in a coil. Four different microstructures are obtained by the following thermomechanical steps:

- Microstructure A: wire straightening, stress relieving (1 h at 873 K, furnace cooling)
- Microstructure B: 1 h at 1193 K followed by furnace cooling, wire straightening, stress relieving
- Microstructure C: 10 h at 1193 K followed by furnace cooling, wire straightening, stress relieving
- Microstructure D: 50 h at 1193 K followed by furnace cooling, wire straightening, stress relieving

The wires are straightened by applying 1% plastic strain in tension. All of the heat treatments are done in vacuum (< 1 x $10^{-3}$ Pa). The stress relieving treatment consists of 1 h at 873 K followed by furnace cooling. Backscattered electron images of polished cross-sections of the four obtained microstructures are shown in Fig. 1. It should be noted that microstructures B, C and D are equiaxed, whereas the grains in microstructure A are elongated along the wire axis. Therefore, a backscattered electron image of the polished longitudinal section of a wire with microstructure A is shown in Fig. 2. The average primary α grain diameter, as determined by electron backscatter diffraction (EBSD) measurements on cross-sections, is approximately 1, 2, 5 and 10 µm for microstructure A, B, C and D, respectively. From tensile tests the 0.2% yield stress is found to be 1056 ± 10 MPa, 873 ± 16 MPa, 830 ± 15 MPa and 850 ± 20 MPa for wires with microstructure A, B, C and D, respectively.

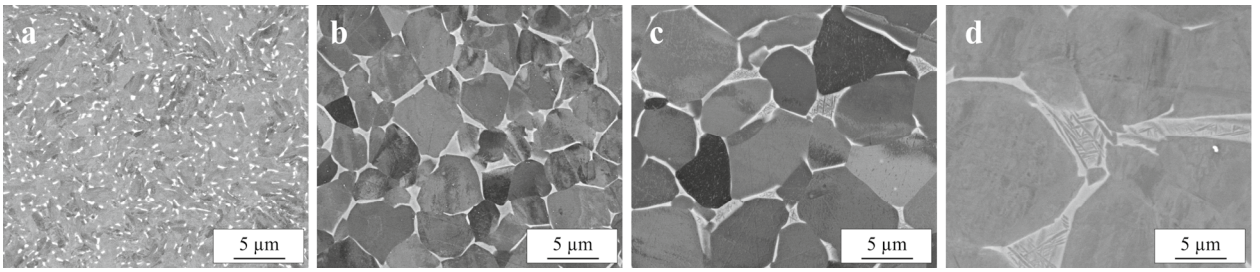


Fig. 1. Backscattered electron images of polished cross-sections of Ti-6Al-4V wires; (a) Microstructure A; (b) Microstructure B; (c) Microstructure C; (d) Microstructure D.

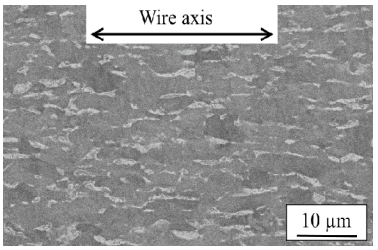


Fig. 2. Backscattered electron image of polished longitudinal section of Ti-6Al-4V wire with microstructure A.

All wires are electrochemically polished for 10 min in an electrolyte containing 550 mL/L $CH_3COOH$, 300 mL/L $H_2SO_4$ and 150 mL/L HF (48% purity) using a current density of 1.2 mA/mm². Further details of this process are described by Pyka et al. (2012). The wires are clamped on each side by grooved titanium plates, which are attached by Araldite Rapid epoxy adhesive. The gauge length, which is approximately 50 mm, is coated with Sicomet 85 cyanoacrylate glue to protect the wire surface. More details on the titanium clamping plate dimensions are described by Everaerts et al. (2016). The wire straightening, tensile testing and fatigue testing are performed on an Instron ElectroPuls E3000. The fatigue testing is load-controlled, with a load ratio of R = 0.1 and a frequency of 60 Hz. A FEI Nova NanoSEM 450 is used for the scanning electron images of microstructures and fracture surfaces. FIB milling and EBSD measurements on the milled surfaces are done using a FEI Nova 600 NanoLab microscope.

## 3. Results and discussion

The fatigue life data of all electrochemically polished samples are shown in Fig. 3. This graph represents, in total, 14 samples with microstructure A, 9 samples with microstructure B, 13 samples with microstructure C and 14 samples with microstructure D. The total testing time for all samples combined is approximately 240 days. In general, the fatigue life decreases if the grain size is increased. For example, at a maximum stress of 750 MPa, all samples with microstructure D break after less than $10^7$ cycles, while most samples with microstructure C do not. At this stress level, some samples with microstructure B do not even break after approximately $10^8$ cycles. A few samples with microstructure A, which has the smallest grain size, do not break after $10^8$ cycles at an even higher maximum stress of 900 MPa. Fractographic examination of the broken samples revealed that four samples, all of which were tested at a maximum stress of 750 MPa, fractured due to an internally initiated crack. In total, seven samples did not break after approximately $10^8$ cycles. A possible explanation for this is the fact that the wire surface was relatively free of defects due to the electrochemical polishing treatment, which delays surface crack initiation and therefore prolongs the fatigue life. This also means that internal cracks could have been initiating in some of these samples, but did not yet reach a critical size.

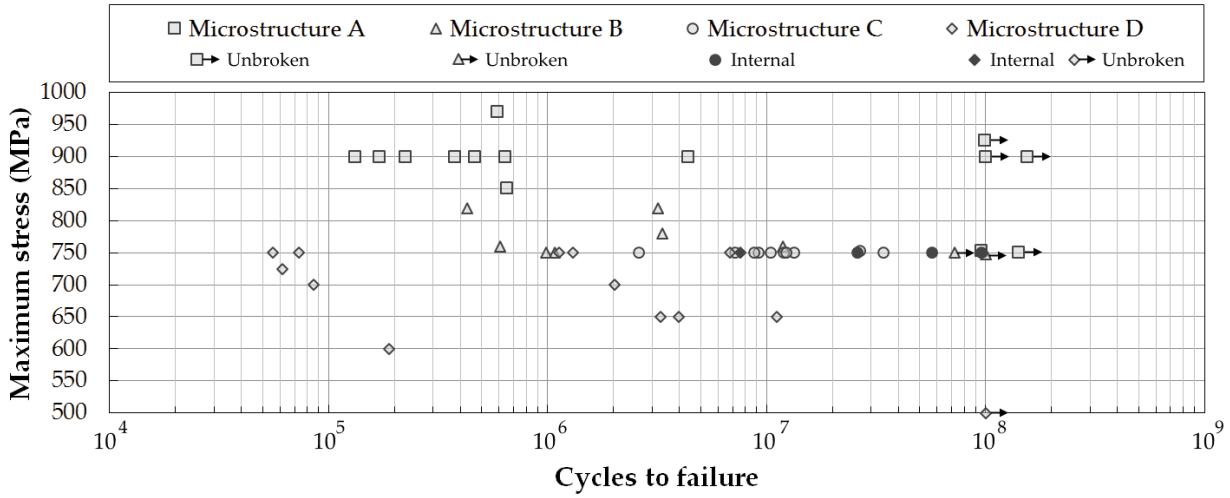


Fig. 3. Fatigue data of electrochemically polished samples with microstructure A, B, C or D, showing the maximum applied stress (MPa) and the resulting cycles to failure; Unbroken samples (7) are represented by symbols with arrows, samples broken due to internal crack initiation (4) are represented by darker symbols; R=0.1.

The fracture surfaces of the four samples that broke due to internal cracks are shown in Fig. 4. The three samples with microstructure C are named C1, C2 and C3, and they failed after 2.6 x $10^7$, 5.7 x $10^7$ and 9.6 x $10^7$ cycles, respectively. The sample with microstructure D, simply named D, failed after 7.6 x $10^6$ cycles. The maximum applied stress for all four samples is 750 MPa. The fracture surface of sample C2 shows a fish-eye type failure, whereas the fracture surfaces of samples C1, C3 and D show a subsurface-type crack. By comparing the fatigue life of sample C2

with that of samples C1 and C3, it can be seen that the distance of the initiation location to the edge does not seem to be correlated to the fatigue life, which is in agreement with the results of Yokoyama et al. (1997). However, sample D, which has a larger grain size, failed after only 7.6 x $10^6$ cycles, which is about an order of magnitude smaller than the fatigue lives of samples C1, C2 and C3. It has been suggested by Zuo et al. (2008) that if dislocation pile-up at grain boundaries is involved in the formation of facets, large α grains can act as weak sites, although the results of fatigue tests on microscale samples performed by Szczepanski et al. (2013) did not support this theory. In any case, because the facets are fractured α grains, a larger grain size results in larger facets. This logically means that if one facet is formed in a microstructure with large grains, it will cause a higher local stress concentration than if one facet is formed in a microstructure with smaller grains. This could explain the much shorter fatigue life of sample D compared to samples C1, C2 and C3, given that the fatigue life is dominated by the crack initiation stage. The crack initiation areas, which are indicated by the white circles in Fig. 4, are very similar for all four samples. These areas contain many facetted α grains, as is illustrated in Fig. 5 for samples C1 and D. Observations of the facets at a higher magnification reveal the presence of nano-roughness or markings, which are to some extent linear in almost all of the facets, as shown in the close-up of Fig. 5a. However, there is one "anomalous" facet in sample D, shown in the close-up in Fig. 5b, on which the markings are not linear but fan-shaped. A very similar pattern was reported by Ivanova et al. (2002), who concluded that it was very likely that this pattern was the result of a cleavage-type fracture mechanism.

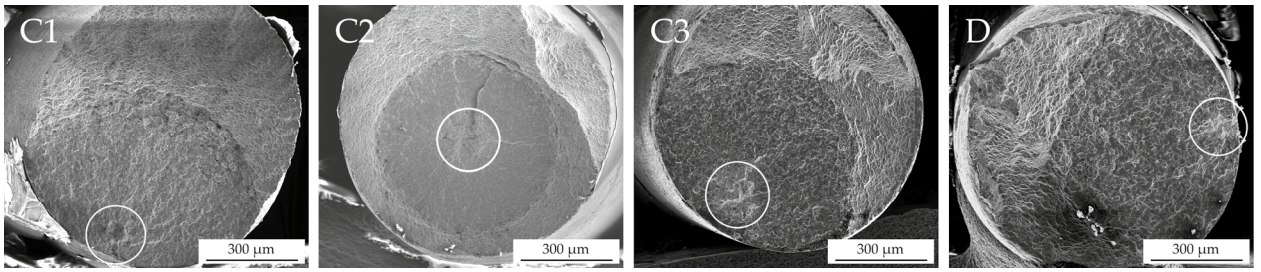


Fig. 4. SEM images of the fracture surfaces of samples that broke after internal crack initiation, white circles indicate the initiation area; Samples C1, C2 and C3, with microstructure C, broke after 2.6 x $10^7$, 5.7 x $10^7$ and 9.6 x $10^7$ cycles at $\sigma_{max}$=750 MPa, respectively; Sample D, with microstructure D, broke after 7.6 x $10^6$ cycles at $\sigma_{max}$=750 MPa.

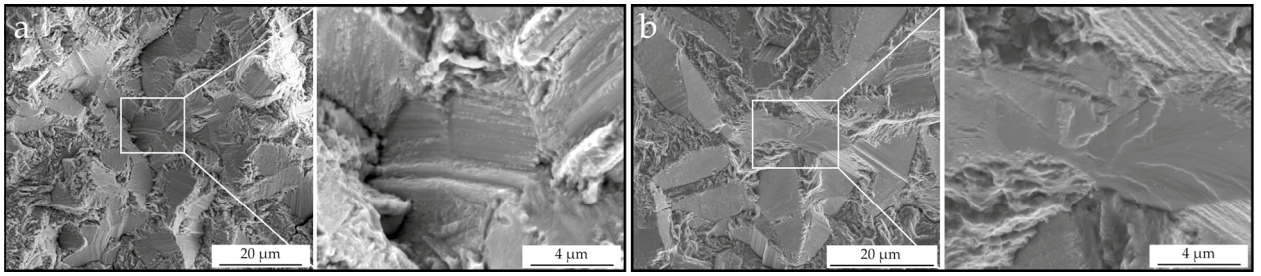


Fig. 5. (a) SEM images of crack initiation area of sample C1 with a close-up of the roughness on a typical facet; (b) SEM images of crack initiation area of sample D with a close-up of the markings on an anomalous facet

The size of the facet-containing area, $area_{fct}$, can be used to estimate the threshold stress intensity factor range for long crack growth, $\Delta K_{th}$. The $area_{fct}$ values are measured from SEM images, by using a freeform selection that encloses all of the facets, as is illustrated in Fig. 6a for sample D. Equation (1), which was derived by Murakami et al. (1989), is used to estimate the threshold stress intensity factor range. In this equation, $\Delta\sigma$ is the difference between the maximum and minimum stress. This equation has been used for internal initiation in Ti-6Al-4V in several publications, although the area parameter is interpreted in different ways. For example, Umezawa and Nagai (1997) used the length of the projected area of the initiation site on the main crack propagation plane instead of the √area parameter, while Xiaolong et al. (2015) used the size of the rough area, approximated by an ellipse. Fig. 6b shows the obtained $\Delta K_{th}$ values as a function of fatigue life for samples D, C1, C2 and C3. These values are between 5 and 6 MPa.$m^{1/2}$, without

an apparent correlation with the fatigue life. In comparison, Xiaolong et al. (2015) reported values between 6 and 8 MPa.m$^{1/2}$ for their own samples, also independent of the fatigue life, and values between 5.9 and 7.3 MPa.m$^{1/2}$ which they calculated from experimental data available in literature. The fact that the values obtained in this study are lower, can be explained by the freeform shape that is used to measure area$_{fct}$. For example, if this area is instead approximated by an ellipse, although there is no apparent physical reason to do so, the $\Delta K_{th}$ value for sample C2 would be 8 MPa.m$^{1/2}$. The microstructure also does not appear to have an influence on the $\Delta K_{th}$ value. However, this observation should be regarded with caution, since there is only one data point for a sample with microstructure D. The disconnection between the $\Delta K_{th}$ values and the fatigue life coupled with the lack of correlation between the location of the initiation and the fatigue life clearly indicates that the fatigue life must be dominated by the initiation stage. In other words, the formation of the cluster of facets takes up most of the fatigue life, until a critical area, area$_{fct}$, is reached, corresponding to the threshold stress intensity factor range for long crack growth.

$$\Delta K_{th} = 0.5 \cdot \Delta\sigma \cdot \sqrt{\pi \sqrt{area_{fct}}} \tag{1}$$

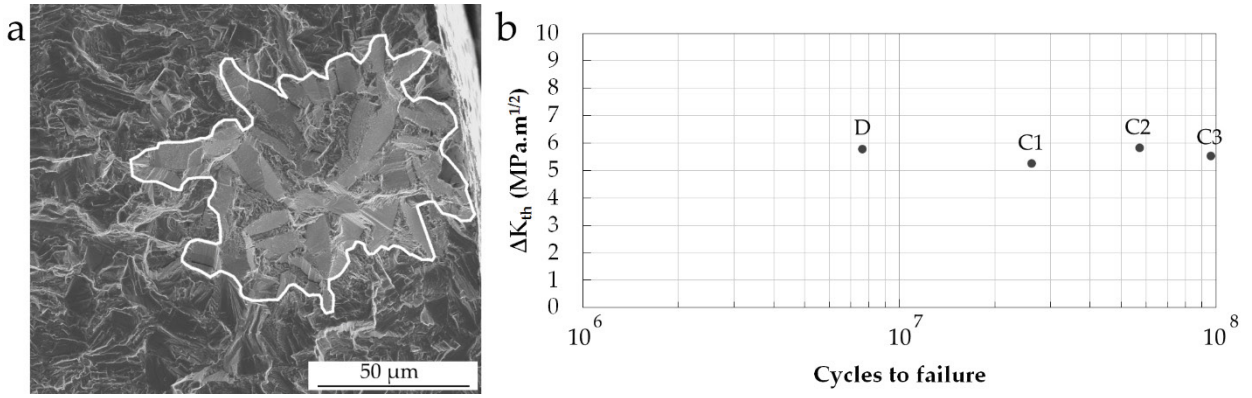


Fig. 6. (a) SEM image of crack initiation area of sample D, which failed after 7.6 x 10$^6$ cycles at $\sigma_{max}$=750 MPa, with the facet-containing area, area$_{FCT}$, outlined by the white line; (b) Threshold stress intensity factor range $\Delta K_{th}$, calculated by equation (1), as a function of fatigue life for samples C1, C2, C3 and D.

It is clear that understanding how the facet-containing area is formed is crucial. If facets are the result of dislocation slip and slip band formation, then they should concur with a certain slip system of the α phase. On the other hand, if they are formed by cleavage, then they should coincide with a cleavage plane. To investigate this, the crystallographic orientation of several facets has been determined by performing EBSD measurements on cross-sections of the fracture surfaces of samples C1 and D, obtained by FIB milling. In total, 10 and 18 facets were analyzed for samples C1 and D, respectively. All of the facets were found to be parallel to a prismatic lattice plane, except for the anomalous facet in sample D (Fig. 5b), which has a near-basal orientation. Fig. 7 illustrates these results for two sections of sample D. In cross section 1 (Fig. 7a, b & c), two regular facets are sectioned and found to be parallel to a prismatic lattice plane. As mentioned earlier, the roughness on these facets has a linear appearance, and Fig. 7e shows that this linearity coincides with the slip direction in the prismatic slip system, which is $<11\bar{2}0>\{10\bar{1}0\}$. These observations strongly suggest that prismatic slip is involved in the formation of these facets. In cross-section 2 (Fig. 7e, f & g), the anomalous facet is sectioned and found to have a near-basal orientation. Wanhill (1973) reported that the cleavage planes in the α phase are consistently found to be planes approximately 15° from the basal $\{0002\}$ plane. The near-basal orientation of the anomalous facet together with the fan-shaped markings (Fig. 5b) suggest that in this case a cleavage mechanism could have caused facet formation. However, it should be pointed out that the near-basal orientation of this facet does not exclude the possibility of basal $<11\bar{2}0>(0002)$ slip, although in that case the presence of the fan-shaped markings, which are totally different from the linear markings on the prismatic facets, cannot be explained.

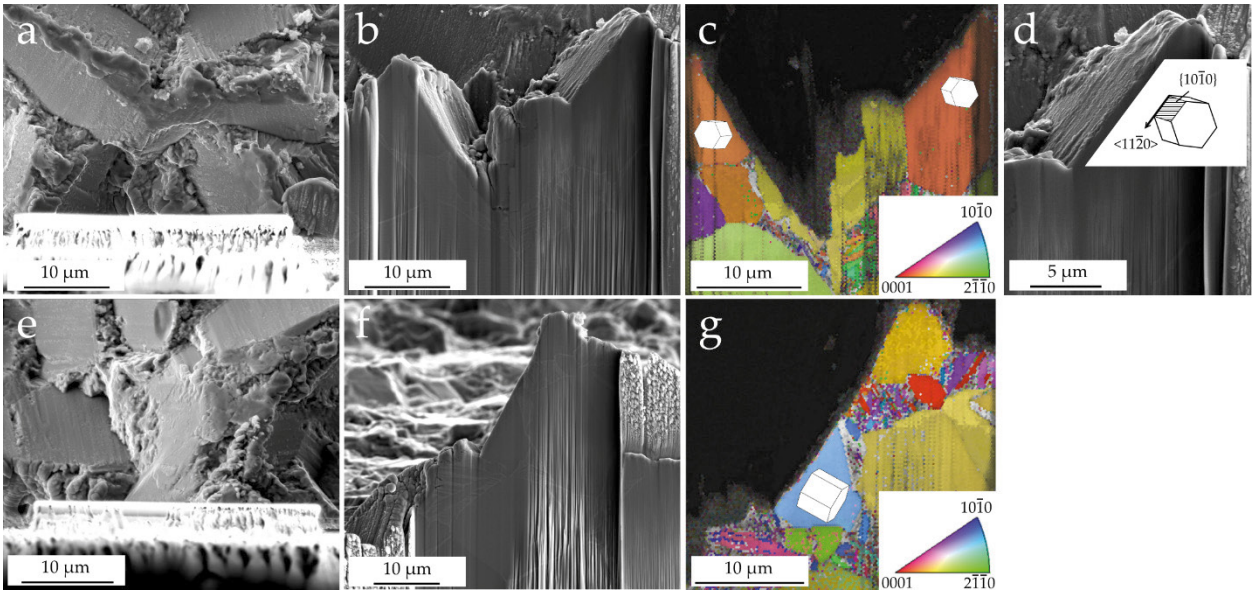


Fig. 7. (a) Top view SEM image of fracture surface of sample D, showing the position of FIB cross-section 1; (b) Front view SEM image of cross-section 1; (c) Color coded orientation map for the α phase obtained by EBSD on cross-section 1, with drawn hexagonal unit cells to illustrate the orientation of the two sectioned facets; (d) Close-up front view SEM image of one of the sectioned facets, illustrating the orientation of the prismatic slip system in this facetted grain; (e) Top view SEM image of fracture surface of sample D, showing the position of FIB cross-section 2; (f) Front view SEM image of cross-section 2; (g) Color coded orientation map for the α phase in cross-section 2, with drawn hexagonal unit cell to illustrate the orientation of the sectioned anomalous facet.

These observations indicate the possibility that there could be two different facet formation mechanisms, one based on slip band formation and one based on cleavage, which would explain the disagreement in literature. Because an anomalous facet was only observed in sample D, and not in samples C1, C2 and C3, it is plausible that the grain size is one of the parameters that controls which mechanism occurs. Additionally, the local crystallographic orientation of the facet and its neighboring grains should be considered, because this determines the local anisotropy and stress field due to dislocation pile-ups. The orientation maps on sectioned facets that were obtained in this study are currently being investigated to clarify the effect of the neighboring grains on the occurrence of facet formation.

## 4. Conclusion

The influence of the alpha grain size on internal fatigue crack initiation in Ti-6Al-4V is investigated by fatigue tests on wires with four different microstructures, with average alpha grain sizes of approximately 1, 2, 5 and 10 µm. Increasing the alpha grain size generally causes a decrease in fatigue life. Four samples broke due to an internal crack: three samples with average alpha grain size 5 µm, which failed after 2.6 x $10^7$, 5.7 x $10^7$ and 9.6 x $10^7$ cycles, and one sample with average alpha grain size 10 µm, which failed after only 7.6 x $10^6$ cycles. The distance of the initiation location to the sample surface is not found to be correlated with the fatigue life. On the fracture surfaces of these four samples a cluster of facets is present at the initiation site. From the size of this facet-containing area, the threshold stress intensity factor range $\Delta K_{th}$ is calculated and found to be between 5 and 6 MPa.$m^{1/2}$ for all four samples. The facets are not smooth, but have some nano-roughness with linear markings for nearly all facets. One anomalous facet, on the fracture surface of the sample with the largest grain size, has a different appearance, with fan-shaped markings. From electron backscatter diffraction measurements on cross-sections of the fracture surfaces, it is found that nearly all of the examined facets are parallel to a prismatic plane of the hexagonal lattice. Additionally, the linear markings coincide with the slip direction of the prismatic slip system. Only the anomalous facet has a near-basal orientation. These observations suggest that it is possible that facets are formed by either a slip-based mechanism or a cleavage-based mechanism, and that the alpha grain size is one of the parameters that controls which mechanism occurs.

## Acknowledgements

The authors acknowledge financial support from the Interuniversity Attraction Poles Program from the Belgian state through the Belgian Policy agency; contract IAP7/21 “INTEMATE”.

## References

Bache, M. R., 1999. Processing titanium alloys for optimum fatigue performance. International Journal of Fatigue 21, S105-S111.

Bathias, C., Drouillac, L., Le Francois, P., 2001. How and why the fatigue S-N curve does not approach a horizontal asymptote. International Journal of Fatigue 23, S143-S151.

Boyer, R. R., 1996. An overview on the use of titanium in the aerospace industry. Materials Science and Engineering A 213(1-2), 103-114.

Bridier, F., Villechaise, P., Mendez, J., 2008. Slip and fatigue crack formation processes in an alpha/beta titanium alloy in relation to crystallographic texture on different scales. Acta Materialia 56(15), 3951-3962.

Dunne, F. P. E., Rugg, D., 2008. On the mechanisms of fatigue facet nucleation in titanium alloys. Fatigue & Fracture of Engineering Materials & Structures 31(11), 949-958.

Everaerts, J., Verlinden, B., Wevers, M., 2016. Internal fatigue crack initiation in drawn Ti-6Al-4V wires. Materials Science and Technology, 'doi:' 10.1080/02670836.2015.1114739.

Furuya, Y., Takeuchi, E., 2014. Gigacycle fatigue properties of Ti-6Al-4V alloy under tensile mean stress. Materials Science and Engineering A 598, 135-140.

Irving, P. E., Beevers, C. J., 1974. Microstructural influences on fatigue crack growth in Ti-6Al-4V. Materials Science and Engineering 14(3), 229-238.

Ivanova, S. G., Biederman, R. R., Sisson, R. D., 2002. Investigation of fatigue crack initiation in Ti-6Al-4V during tensile-tensile fatigue. Journal of Materials Engineering and Performance 11(2), 226-231.

Jha, S. K., Szczepanski, C. J., Golden, P. J., Porter, W. J., John, R., 2012. Characterization of fatigue crack-initiation facets in relation to lifetime variability in Ti-6Al-4V. International Journal of Fatigue 42, 248-257.

Kazymyrovych, V., 2009. Very high cycle fatigue of engineering materials: A literature review. Karlstad University Studies 22.

Liu, X., Sun, C., Hong, Y., 2016. Faceted crack initiation characteristics for high-cycle and very-high-cycle fatigue of a titanium alloy under different stress ratios. International Journal of Fatigue, 'doi:' 10.1016/j.ijfatigue.2016.03.013.

Murakami, Y., Kodama, S., Konuma, S., 1989. Quantitative-evaluation of effects of non-metallic inclusions on fatigue-strength of high-strength steels. I:Basic fatigue mechanism and evaluation of correlation between the fatigue fracture-stress and the size and location of non-metallic inclusions. International Journal of Fatigue 11(5), 291-298.

Neal, D. F., Blenkinsop, P. A., 1976. Internal fatigue origins in alpha-beta titanium-alloys. Acta Metallurgica 24(1), 59-63.

Oguma, H., Nakamura, T., 2010. The effect of microstructure on very high cycle fatigue properties in Ti-6Al-4V. Scripta Materialia 63(1), 32-34.

Paton, N. E., Williams, J. C., Chesnutt, J. C., Thompson, A. W., 1975. The effects of microstructure on the fatigue and fracture of commercial titanium alloys. AGARD Conference Proceedings 185, 4-1 - 4-14.

Pilchak, A. L., Bhattacharjee, A., Rosenberger, A. H., Williams, J. C., 2009. Low Delta K faceted crack growth in titanium alloys. International Journal of Fatigue 31(5), 989-994.

Pyka, G., Burakowski, A., Kerckhofs, G., Moesen, M., Van Bael, S., Schrooten, J., Wevers, M., 2012. Surface Modification of Ti6Al4V Open Porous Structures Produced by Additive Manufacturing. Advanced Engineering Materials 14(6), 363-370.

Szczepanski, C. J., Jha, S. K., Shade, P. A., Wheeler, R., Larsen, J. M., 2013. Demonstration of an in situ microscale fatigue testing technique on a titanium alloy. International Journal of Fatigue 57, 131-139.

Umezawa, O., Nagai, K., 1997. Subsurface crack generation in high-cycle fatigue for high strength alloys. Isij International 37(12), 1170-1179.

Wanhill, R. J. H., 1973. Consideration of cleavage in alpha titanium. Acta Metallurgica 21(9), 1253-1258.

Wu, G. Q., Shi, C. L., Sha, W., Sha, A. X., Jiang, H. R., 2013. Effect of microstructure on the fatigue properties of Ti-6Al-4V titanium alloys. Materials & Design 46, 668-674.

Xiaolong, L., Chengqi, S., Youshi, H., 2015. Effects of stress ratio on high-cycle and very-high-cycle fatigue behavior of a Ti-6Al-4V alloy. Materials Science and Engineering A 622, 228-235.

Yokoyama, H., Umezawa, O., Nagai, K., Suzuki, T., 1997. Distribution of internal crack initiation sites in high-cycle fatigue for titanium alloys. Isij International 37(12), 1237-1244.

Zuo, J. H., Wang, Z. G., Han, E. H., 2008. Effect of microstructure on ultra-high cycle fatigue behavior of Ti-6Al-4V. Materials Science and Engineering A 473(1-2), 147-152.